Supporting Information

Redox-responsive Polysulfide-based Biodegradable Organosilica Nanoparticles for Delivery of Bioactive Agents

Seyyed Pouya Hadipour Moghaddam [a, b], Jiban Saikia [b], Mostafa Yazdimamaghani [a, b], and Hamidreza Ghandehari [a, b, c, *]

[a] *Department of Pharmaceutics and Pharmaceutical Chemistry, University of Utah, Salt Lake City, UT 84112, USA*

[b] *Utah Center for Nanomedicine, Nano Institute of Utah, University of Utah, Salt Lake City, UT 84112, USA*

[c] *Department of Bioengineering, University of Utah, Salt Lake City, UT 84112, USA*

[*] *Corresponding Author. Utah Center for Nanomedicine, Nano Institute of Utah, 5205 SMBB, 36 S. Wasatch Dr, Salt Lake City, UT 84112, USA*

Email Address: hamid.ghandehari@utah.edu (H. Ghandehari)

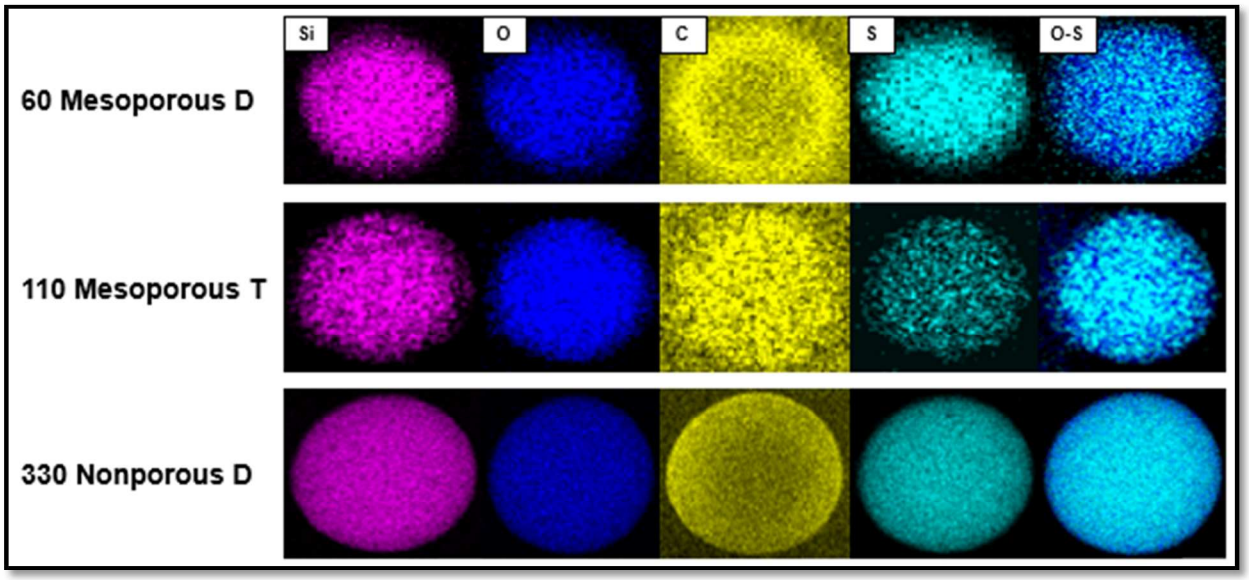

Figure S1. STEM images for 60 Mesoporous D, 110 Mesoporous T, and 330 Nonporous D nanoparticles.

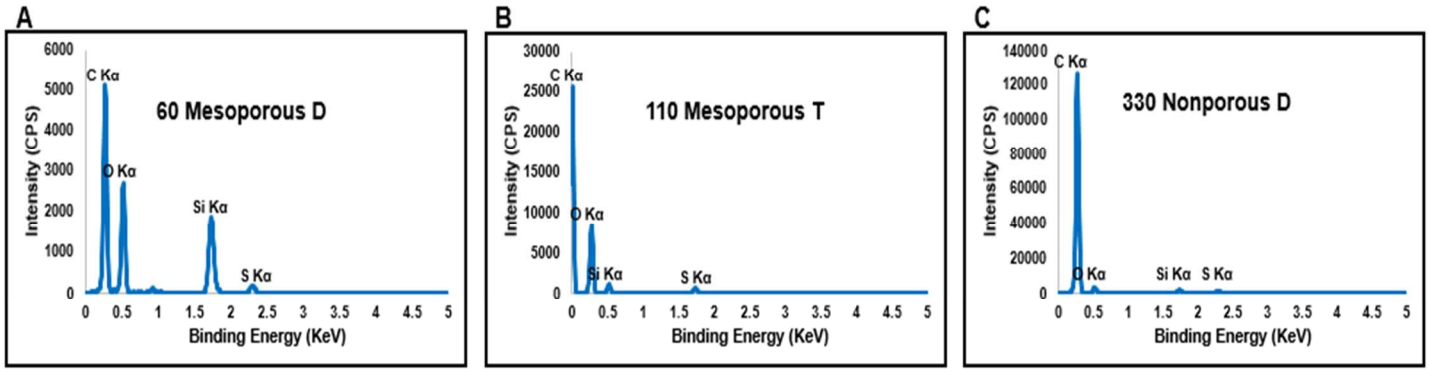

Figure S2. STEM spectra of (A) 60 Mesoporous D; (B) 110 Mesoporous T; and (C) 330 Nonporous D nanoparticles.

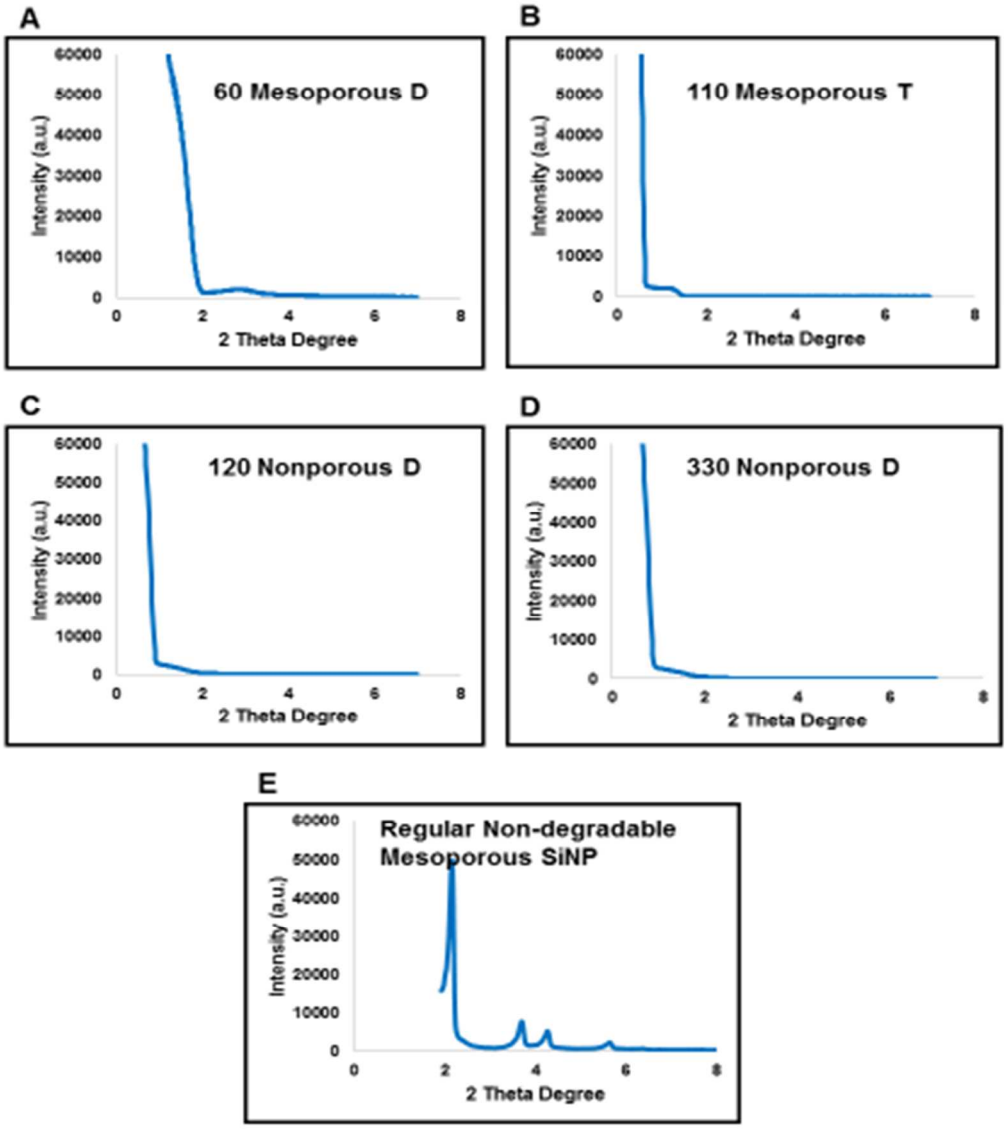

Figure S3. XRD graphs for (A) 60 Mesoporous D; (B) 110 Mesoporous T; (C) 120 Nonporous D; (D) 330 Nonporous D; and (E) regular non-degradable mesoporous SiNP. The degradable mesoporous nanoparticles did not exhibit the typical Bragg peaks like regular non-degradable mesoporous SiNP.

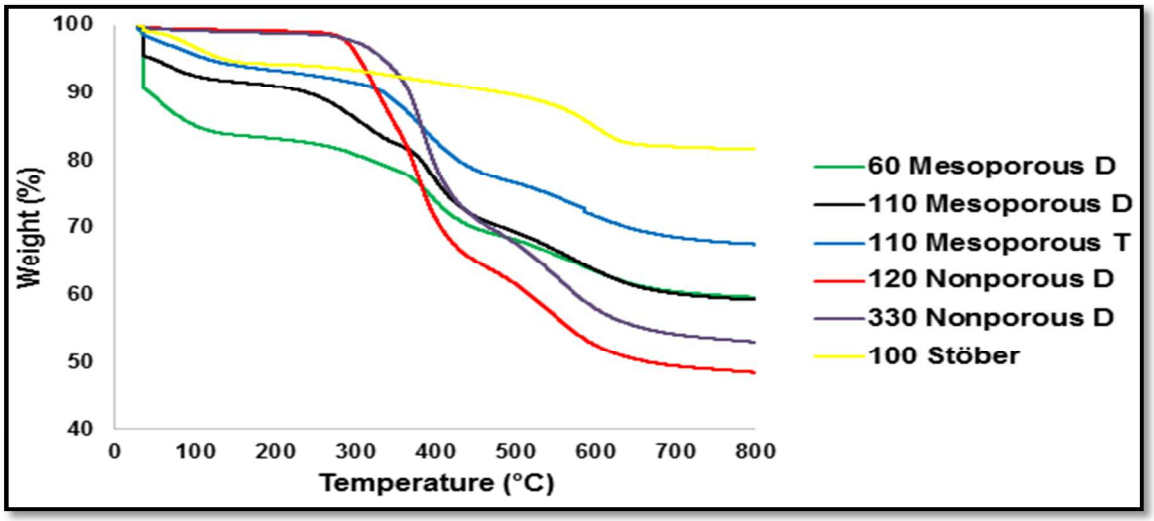

Figure S4. TGA analyses for the synthesized nanoparticles. Stöber 100 SiNP was used as a control.

A

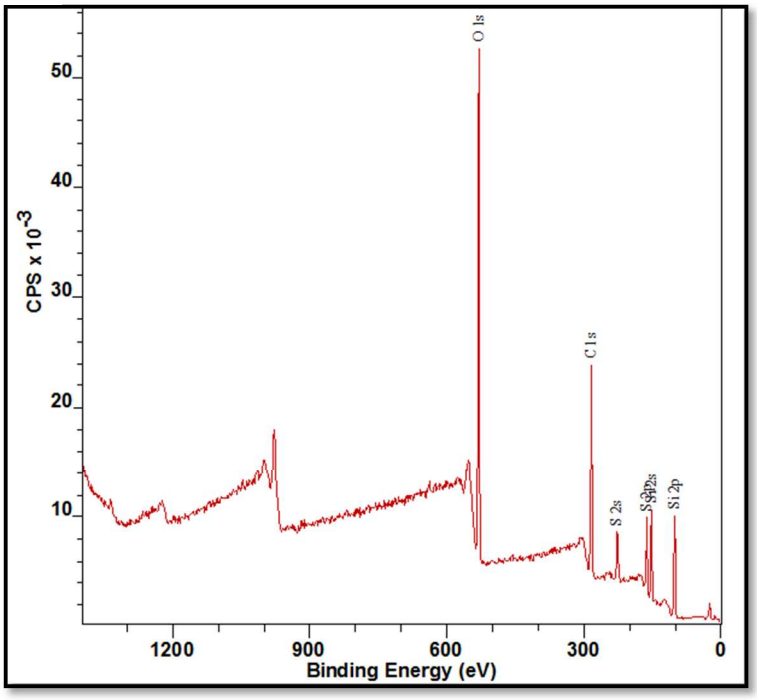
O 1s
C 1s
S 2s
S 2p
Si 2p
CPS x 10^-3
50
40
30
20
10
1200
900
600
300
0
Binding Energy (eV)

B

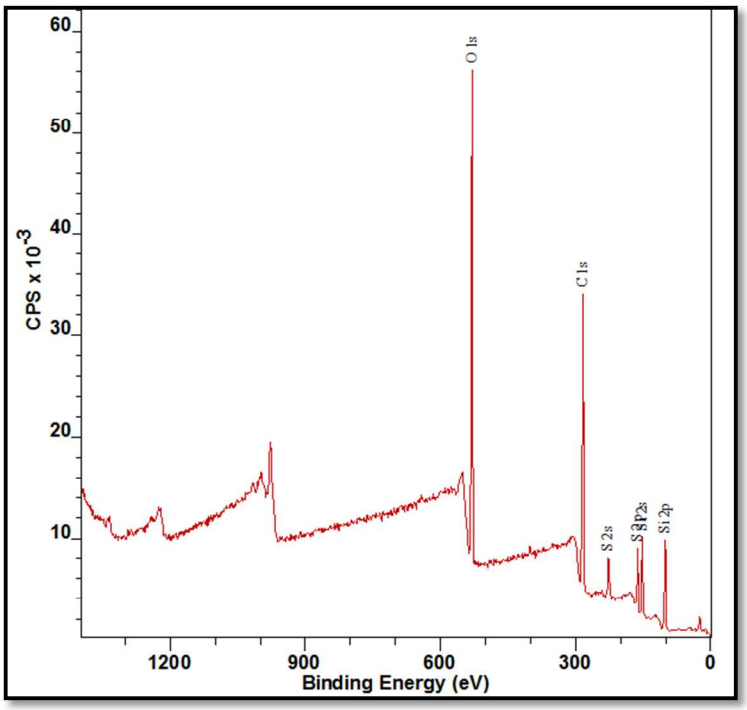
O 1s
C 1s
S 2s
S 2p
Si 2p
CPS x 10^-3
60
50
40
30
20
10
1200
900
600
300
0
Binding Energy (eV)

C

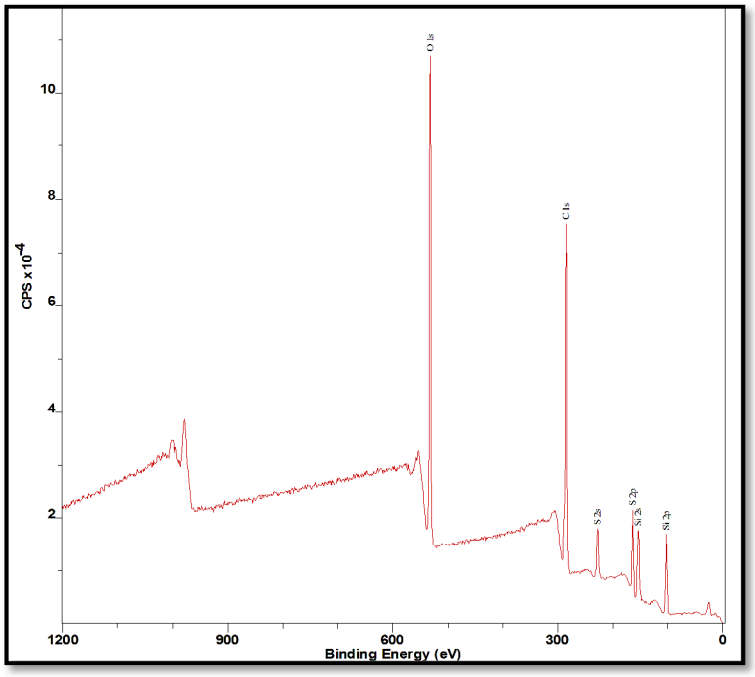
O 1s
C 1s
S 2s
Si 2s
S 2p
Si 2p
CPS x 10^-4
10
8
6
4
2
1200
900
600
300
0
Binding Energy (eV)

D

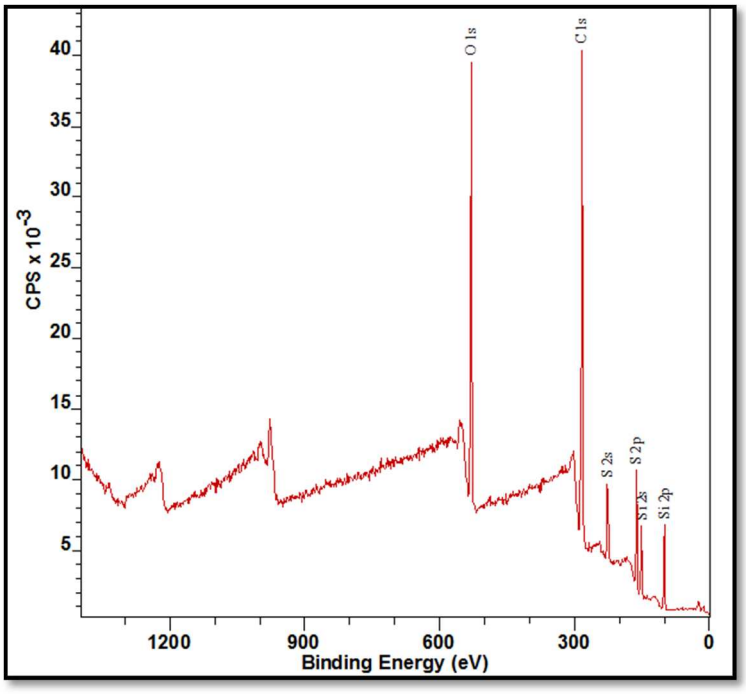
O 1s
C 1s
S 2s
S 2p
Si 2s
Si 2p
CPS x 10^-3
40
35
30
25
20
15
10
5
1200
900
600
300
0
Binding Energy (eV)

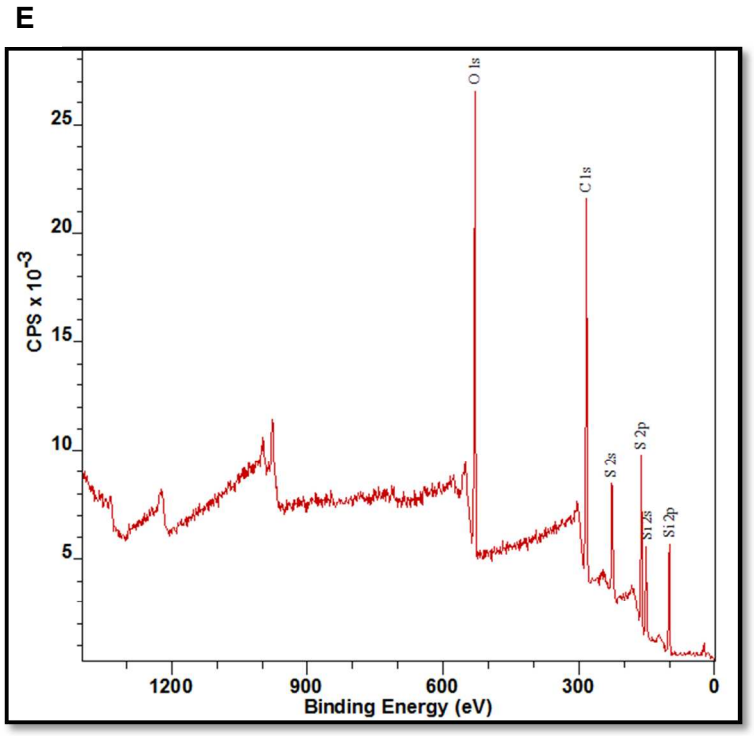

Figure S5. XPS survey spectra of (A) 60 Mesoporous D; (B) 110 Mesoporous D; (C) 110 Mesoporous T; (D) 120 Nonporous D; and (E) 330 Nonporous D nanoparticles.

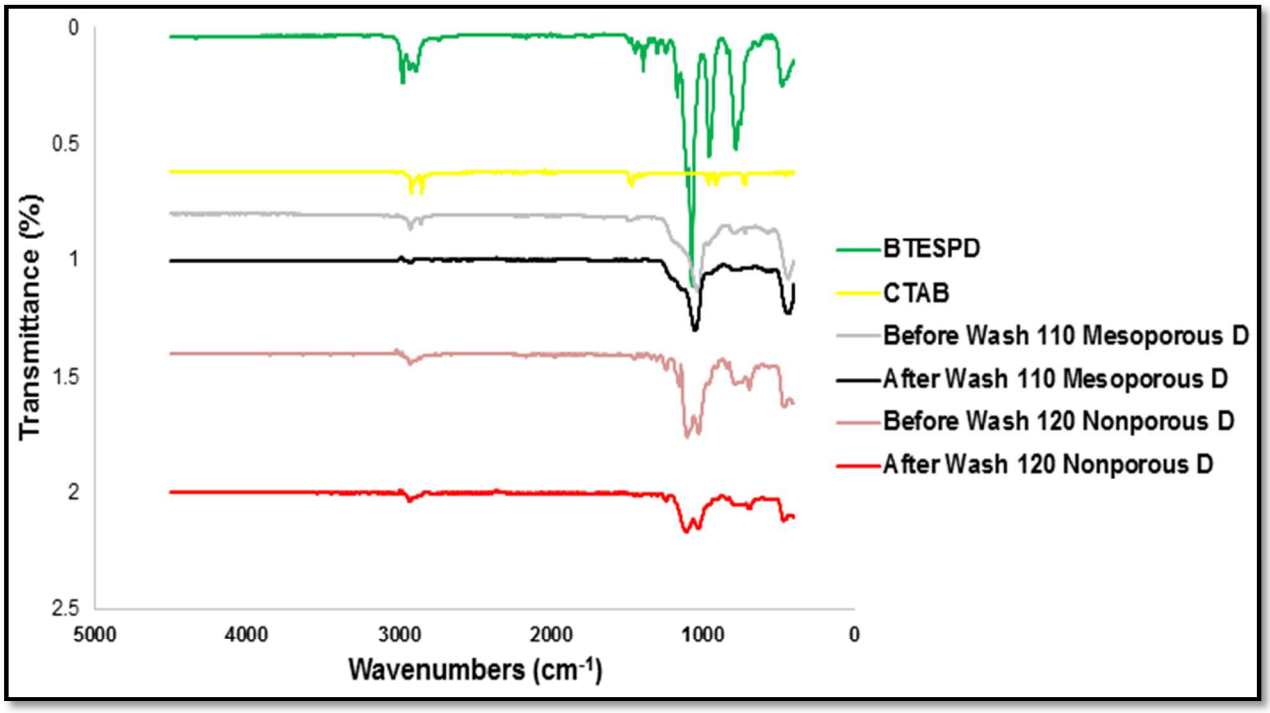

Figure S6. FTIR spectra of 110 Mesoporous D and 120 Nonporous D nanoparticles before and after washing. CTAB and BTESPD (disulfide-based precursor) were also analyzed for better comparison. Typical CTAB peaks around 3000 cm^{-1} were not seen after washing the nanoparticles. This confirms complete removal of the surfactant from the pores.

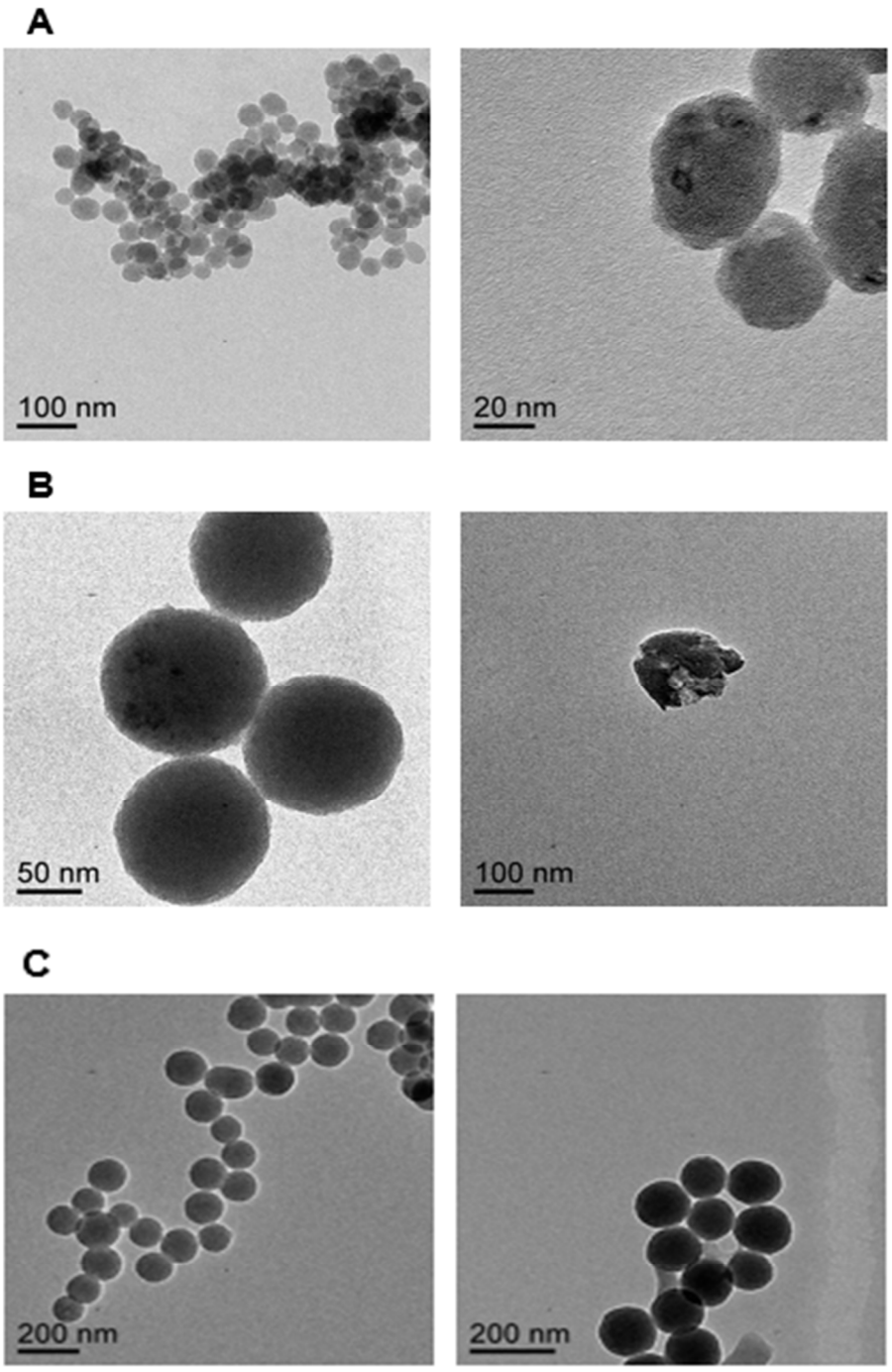

Figure S7. Degradation images of mesoporous nanoparticles after 15 days in the presence of 8 μM GSH; (A) 60 Mesoporous D; (B) 110 Mesoporous D; and (C) 110 Mesoporous T nanoparticles.

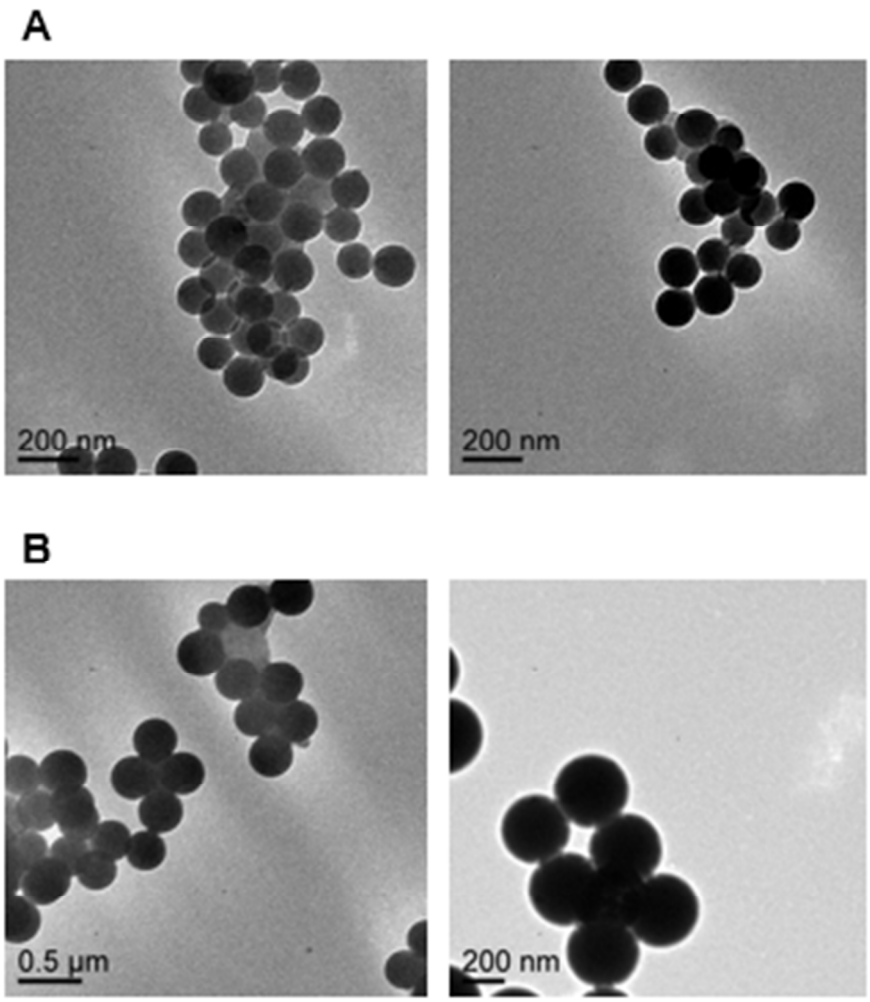

Figure S8. Degradation images of nonporous nanoparticles after 15 days in the presence of 8 μM GSH; (A) 120 Nonporous D and (B) 330 Nonporous D nanoparticles.

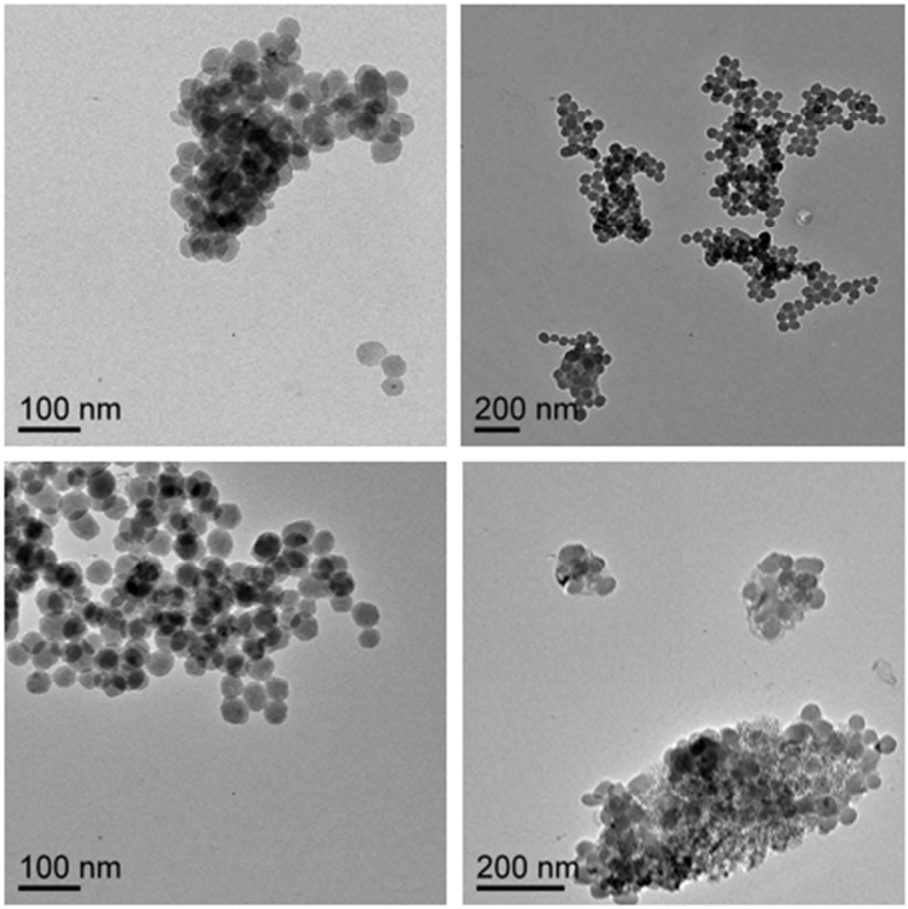

Figure S9. Agglomeration of 60 Mesoporous D nanoparticles in solution containing 8 mM GSH.

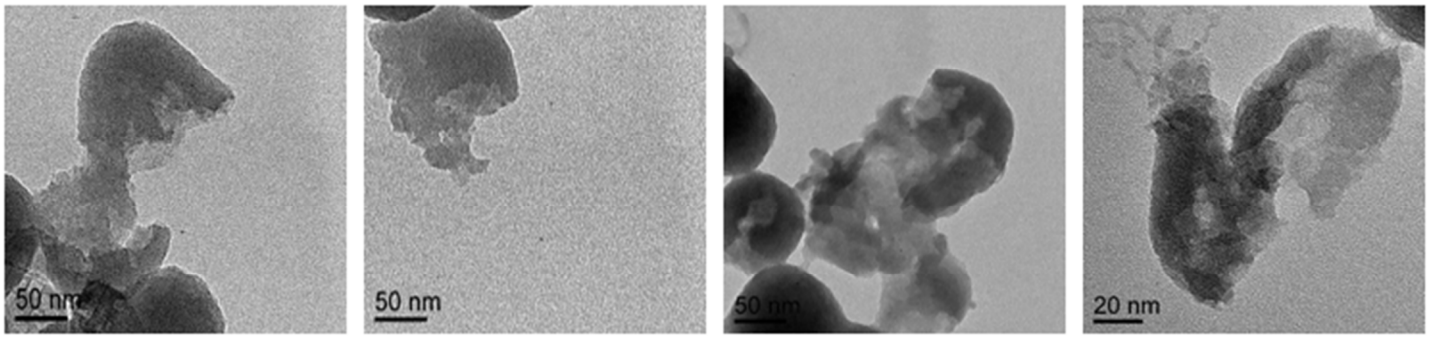

Figure S10. Degradation of 110 Mesoporous D nanoparticles after 48 h in the presence of 8 mM GSH.

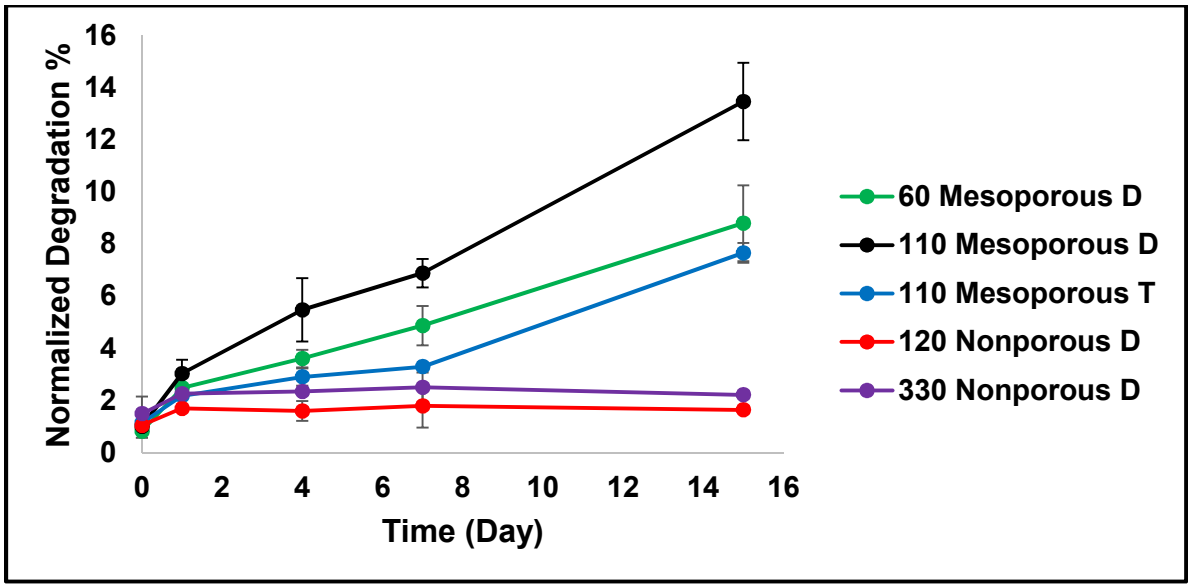

Figure S11. Normalized degradation percentages of all synthesized nanoparticles over the 15-day period of study.

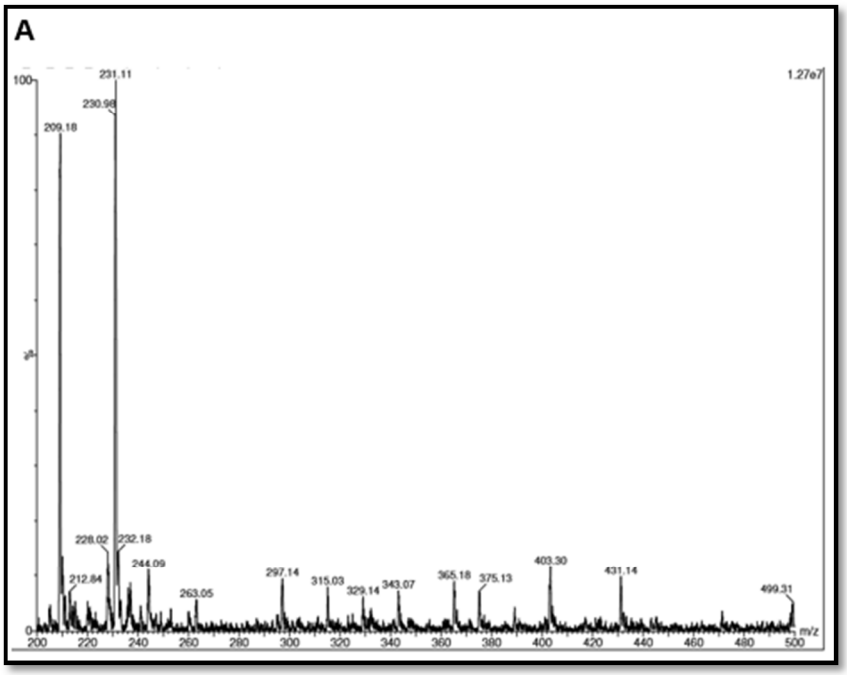
A
100
%
0
231.11
230.98
209.18
228.02
232.18
212.84
244.09
263.05
297.14
315.03
329.14
343.07
365.18
375.13
403.30
431.14
499.31
1.27e7
200 220 240 260 280 300 320 340 360 380 400 420 440 460 480 500
m/z

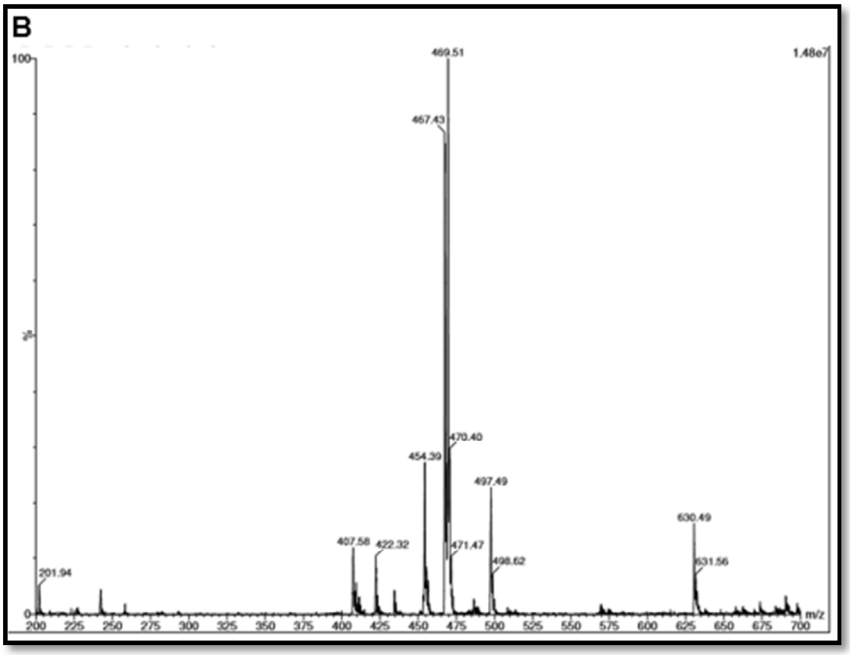
B
100
%
0
469.51
467.43
470.40
454.39
497.49
630.49
407.58
422.32
471.47
498.62
631.56
201.94
1.48e7
200 225 250 275 300 325 350 375 400 425 450 475 500 525 550 575 600 625 650 675 700
m/z

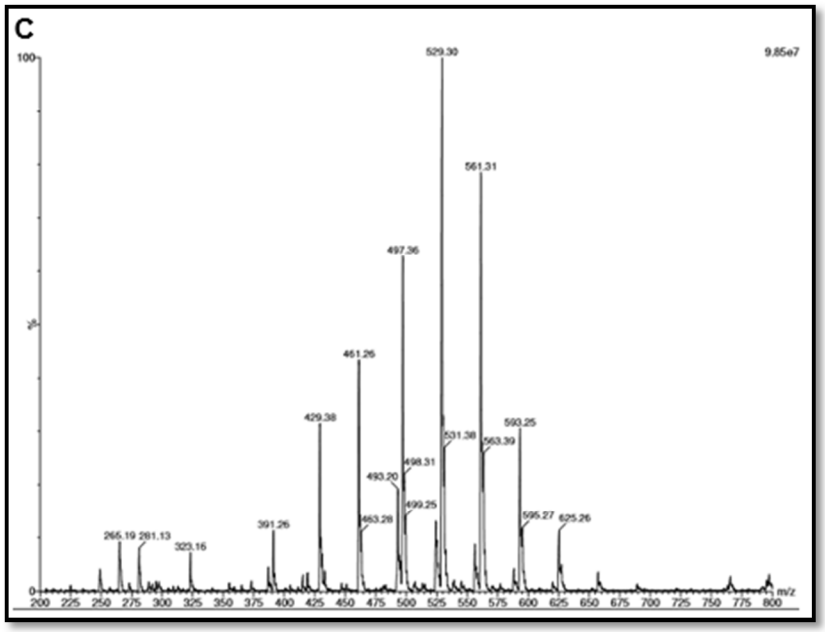
C
9.85e7
529.30
561.31
497.36
461.26
429.38
531.38
593.25
563.39
498.31
493.20
499.25
463.28
595.27
625.26
391.26
266.19
281.13
323.16
%
m/z

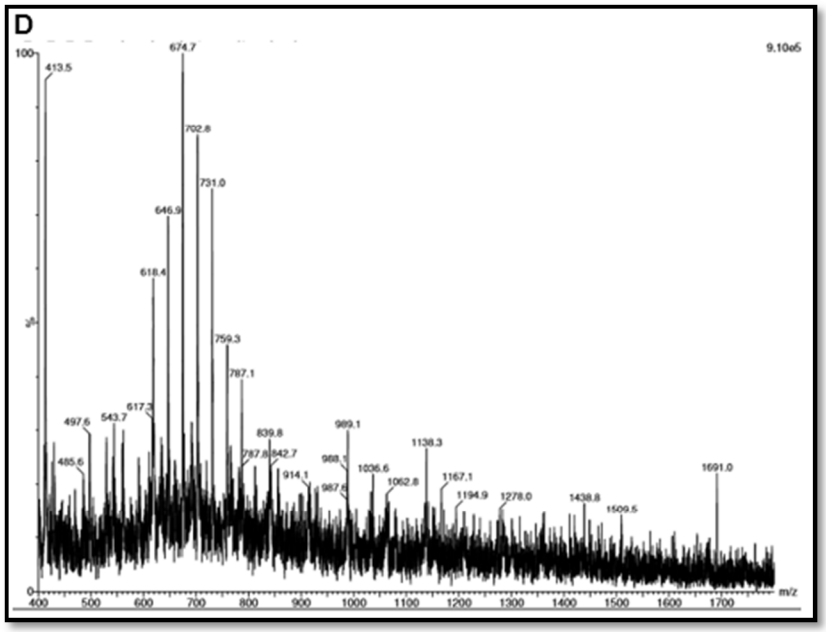
D
9.10e6
674.7
413.5
702.8
731.0
646.9
618.4
759.3
787.1
497.6
543.7
839.8
989.1
1138.3
1691.0
%
m/z

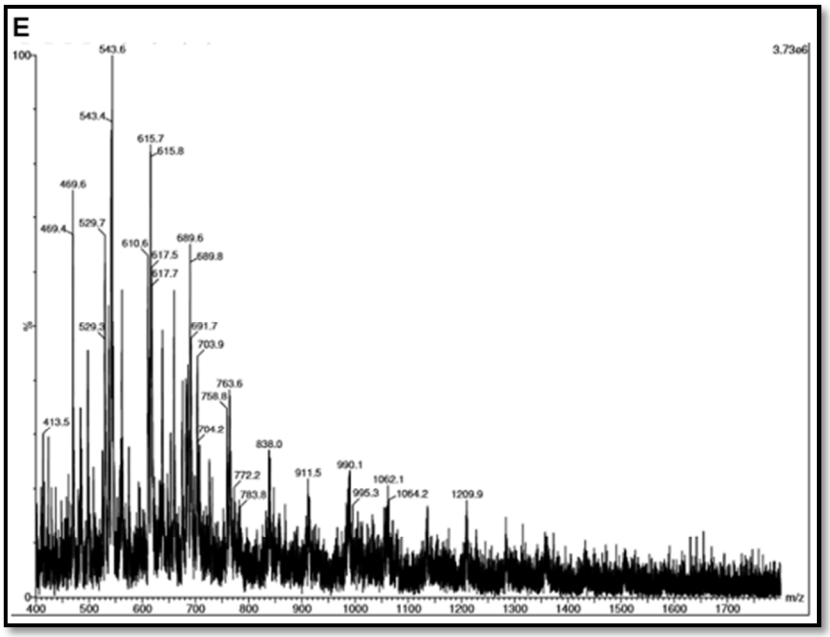
E
3.73e6
100
%
0
543.6
543.4
615.7
615.8
469.6
469.4
529.7
610.6
689.6
617.5
689.8
617.7
529.3
691.7
703.9
763.6
758.8
413.5
704.2
838.0
772.2
911.5
990.1
783.8
995.3
1062.1
1064.2
1209.9
400 500 600 700 800 900 1000 1100 1200 1300 1400 1500 1600 1700
m/z

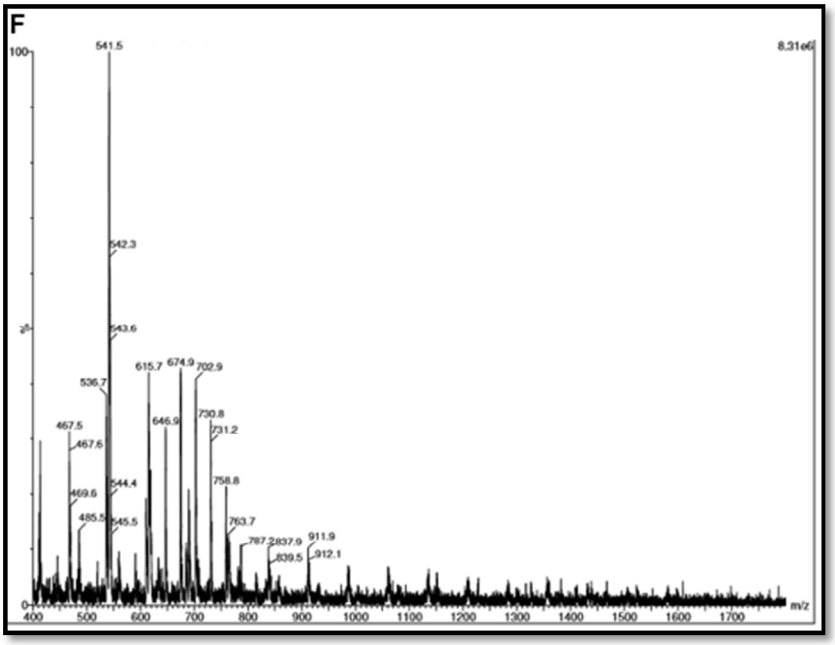
F
8.31e6
100
%
0
541.5
542.3
543.6
615.7
674.9
702.9
536.7
730.8
646.9
731.2
467.5
467.6
758.8
544.4
469.6
763.7
485.5
545.5
787.2
837.9
911.9
839.5
912.1
400 500 600 700 800 900 1000 1100 1200 1300 1400 1500 1600 1700
m/z

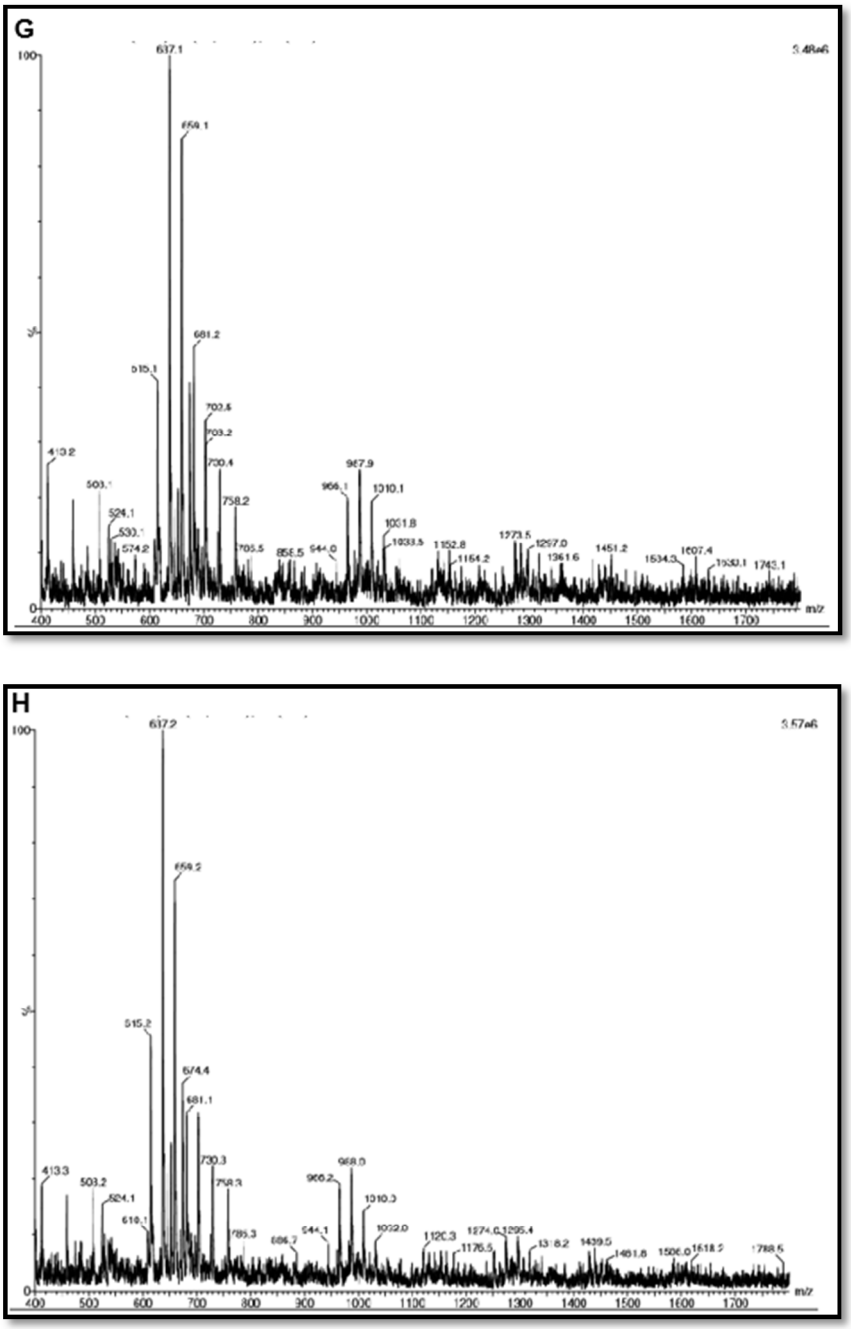

Figure S12. ESI-MS for 3 precursors: (A) TEOS; (B) BTESPD; and (C) BTESPT. ESI-MS for the degradation products: (D) 60 Mesoporous D; (E) 110 Mesoporous D; (F) 110 Mesoporous T; (G) 120 Nonporous D; and (H) 330 Nonporous D nanoparticles.

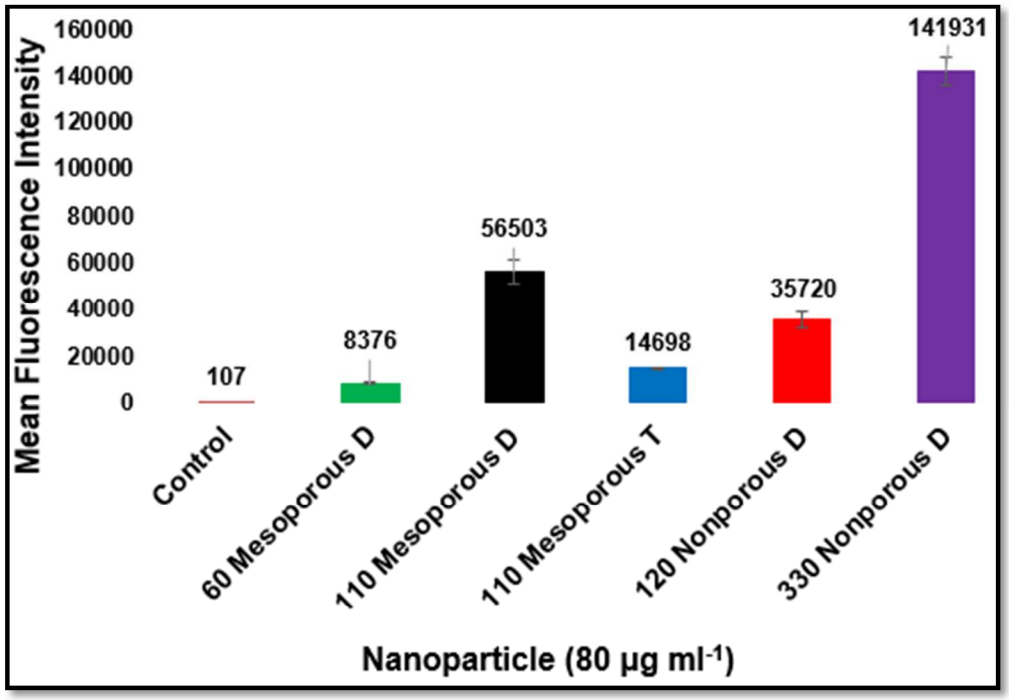

Figure S13. Nanoparticle uptake comparison *via* flow cytometry in RAW 264.7 macrophages after 24 h incubation with the concentration of 80 μg ml^{-1}. Data are mean ± SD (n = 3).

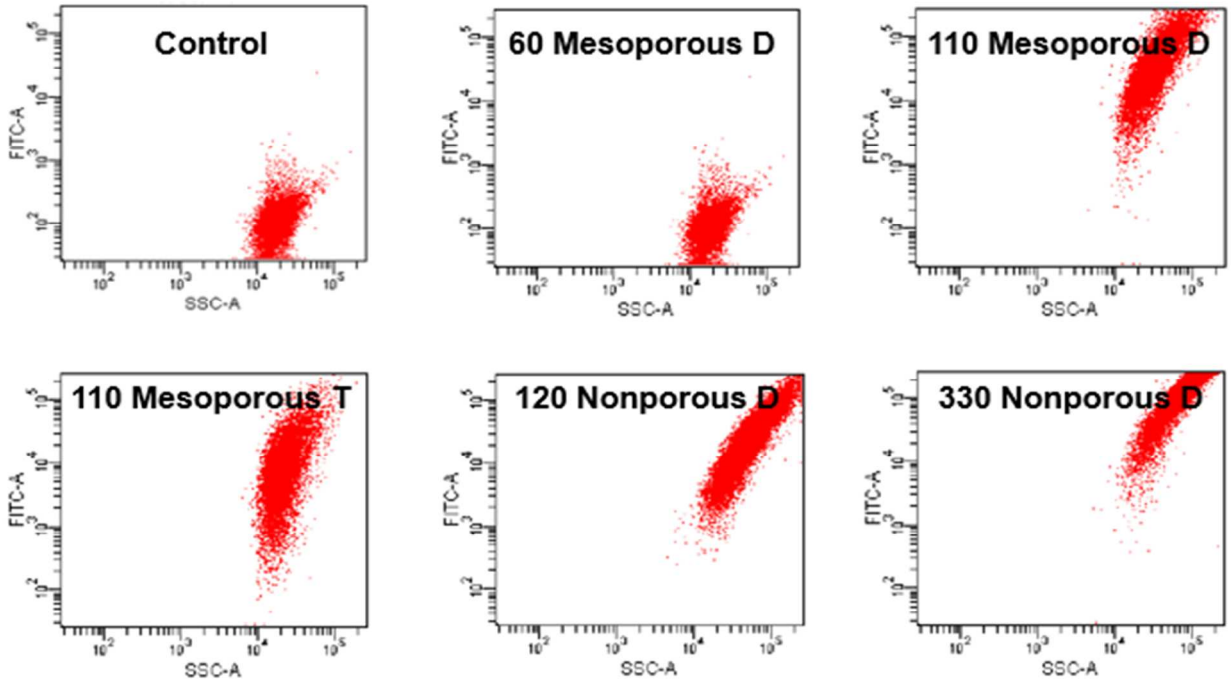

Figure S14. Dot plots from flow cytometry analyses of RAW 264.7 macrophages after 24 h incubation with 80 μg ml^{-1} nanoparticles.

Table S1. Atomic (top) and mass (bottom) percentages of the synthesized nanoparticles measured by XPS

Nanoparticle	O	C	S	Si
60 Mesoporous D	30.69	44.67	6.72	17.92
110 Mesoporous D	26.91	54.88	4.68	13.53
110 Mesoporous T	24.6	62	2.20	11.20
120 Nonporous D	19.07	56.73	11.39	12.81
330 Nonporous D	17.66	67.12	6.73	8.49
100 Stöber	31.01	56.14	0	12.84

Nanoparticle	O	C	S	Si
60 Mesoporous D	28.11	30.72	12.37	28.80
110 Mesoporous D	26.58	40.70	9.26	23.47
110 Mesoporous T	25.86	48.89	4.62	20.60
120 Nonporous D	17.82	39.81	21.34	21.03
330 Nonporous D	18.31	52.26	13.98	15.45
100 Stöber	32.40	44.04	0	23.56